Nitrogen Cycling

https://doi.org/10.48130/nc-0025-0018

Original Research

Open Access

A large net source revealed by the atmospheric reactive nitrogen budget in a subtropical plateau lake basin, southwest China

Qikun Shen[1#], Bowen Tang[1#], Xinyu Wu[1#], Jiahui Kang[1], Jiawei Li[2], Yuepeng Pan[3], Xuejun Liu[1] and Wen Xu[1*]

Received: 25 October 2025

Revised: 30 November 2025

Accepted: 19 December 2025

Published online: 19 January 2026

Abstract

Quantifying the source–sink budget of atmospheric reactive nitrogen (N_r) is crucial for mitigating N_r pollution in vulnerable lake ecosystems. Here, a comprehensive analysis of the atmospheric N_r budget in the Erhai Lake Basin (ELB) (a subtropical plateau lake in southwestern China) is presented. Emission of ammonia (NH_3) and nitrogen oxides (NO_x) for 2022 emissions were estimated using detailed activity data and localized emission factors, while dry and wet N_r deposition in 2023 was quantified through a nine-site monitoring network. The one-year difference, necessitated by data availability, does not affect the core conclusions, given the stability of the fundamental emission source structure. Total atmospheric N_r emissions were estimated at 10,720.4 t N yr^{-1}, dominated by NO_x-N (55.6%), followed by NH_3-N (44.4%). Agriculture was the primary source of NH_3-N (91.7%), with nearly equal contributions from livestock (48.9%) and fertilization (42.8%). In contrast, the transportation sector dominated NO_x-N emissions (98.2%). Annual N_r deposition averaged 10.4 kg N ha^{-1} yr^{-1}, predominantly in the reduced form (NH_x-N, 68.9%). The net atmospheric N_r budget revealed a substantial surplus of 8,201.2 t N yr^{-1}, unequivocally identifying the ELB as a significant net source. The present results underscore the imperative for integrated mitigation strategies that concurrently address emissions from agricultural and vehicles to alleviate regional N_r pollution.

Keywords: Nitrogen cycling, Ammonia emissions, Nitrogen oxides, Atmospheric deposition, Source-sink budget, Erhai Lake basin

Highlights

- The Erhai Lake Basin is a net atmospheric nitrogen source with an 8.2 kt N yr^{-1} surplus.
- Agriculture dominates NH_3 emissions, while vehicles lead NO_x emissions.
- Reduced nitrogen (NH_x) dominates deposition, accounting for 68.9%.
- Low local deposition implies significant potential for long-range transport.

# Authors contributed equally: Qikun Shen, Bowen Tang and Xinyu Wu

* Correspondence: Wen Xu (wenxu@cau.edu.cn)

Full list of author information is available at the end of the article.

https://doi.org/10.48130/nc-0025-0018

Graphical abstract

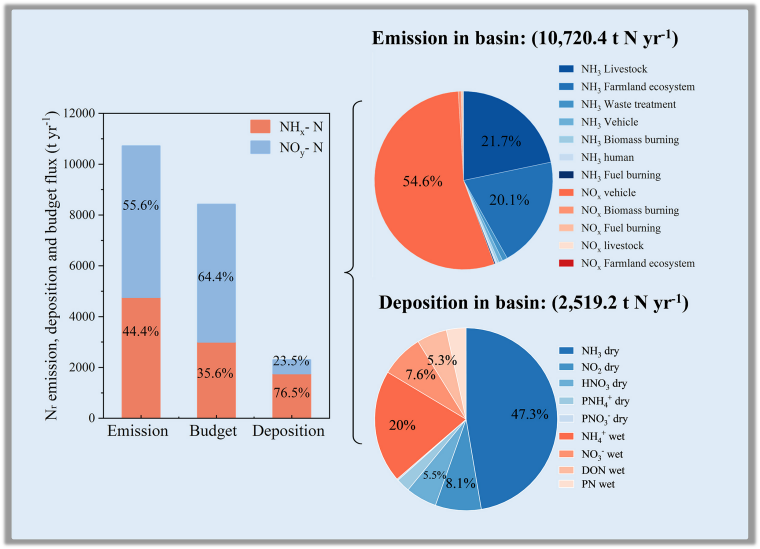

Introduction

Atmospheric reactive nitrogen (N_r) comprises a suite of biologically, photochemically, and radiatively active nitrogen compounds, including inorganic species like ammonia (NH_3), nitrogen oxides (NO_x), nitric acid (HNO_3), particulate ammonium (NH_4^+), and nitrate (NO_3^-), and organic nitrogen. These compounds exert profound impacts on atmospheric chemistry and ecosystem functioning[1]. As the principal atmospheric alkaline gas, NH_3 readily neutralizes acidic species such as HNO_3 and H_2SO_4 to form secondary inorganic aerosols (SIAs), including ammonium sulfate ($(NH_4)_2SO_4$) and ammonium nitrate (NH_4NO_3)[2,3]. These SIAs are dominant components of fine particulate matter ($PM_{2.5}$), contributing up to 40% or more of its mass n polluted regions[4,5]. Concurrently, NO_x ($NO + NO_2$) is a key precursor to tropospheric ozone and secondary organic aerosols, posing significant risks to human health and contributing to climate change[6]. Moreover, excessive deposition of N_r onto terrestrial and aquatic ecosystems through wet and dry pathways can lead to soil acidification, water eutrophication, and biodiversity loss[7,8].

The atmospheric N_r budget, governed by the balance between emission and deposition fluxes, has been profoundly perturbed over the past century by intensified agricultural and industrial activities[9]. In China, the rapid escalation in synthetic fertilizer use and fossil fuel combustion from the 1980s to the 2010s resulted in a dramatic surge in NH_3 and NO_x emissions, establishing the nation as a global hotspot for atmospheric N_r[10]. In response, stringent national air quality policies, including the Clean Air Action (2013–2017) and the Three-Year Action Plan for Winning the Blue-Sky Defense Battle (2018–2020), were implemented. These policies successfully curtailed NO_x emissions, particularly from the industrial and transportation sectors, leading to a 59% reduction in national emissions by 2017 relative to 2010 levels[11]. In contrast, NH_3 emissions, derived mainly from agricultural activities, remained stable or even increased slightly over the same period, owing to a comparative lack of regulatory focus[11]. This divergent emission trajectory has consequently reshaped atmospheric deposition patterns, as evidenced by data from the Nationwide Nitrogen Deposition Monitoring Network (NNDMN), which indicate a rising ratio of reduced to oxidized nitrogen deposition between 2010 and 2020[12,13]. Parallel successes in reducing NO_x emissions and deposition in Europe and North America further affirm the tight coupling between emissions and deposition[14], highlighting the need for a synergistic approach to investigating the complete atmospheric nitrogen budget.

Accurate quantification of the atmospheric nitrogen budget is fundamental for identifying regional N_r sources and sinks and for designing targeted mitigation strategies[15,16]. Bottom-up emission inventories, which integrate sector-specific activity data with regionally approximate emission factors, serve as a primary tool for estimating anthropogenic N_r emissions and have been progressively refined[17–19]. Concurrently, diverse methodologies, including field monitoring, satellite remote observations, and chemical transport modeling, have been employed to quantify atmospheric N_r deposition via wet and dry pathways[20]. While wet deposition (the flux of N_r in precipitation) is relatively straightforward to measure, quantifying dry deposition remains methodologically challenging due to the multitude of contributing gaseous and particulate N_r species and their species-dependent deposition velocities[20]. A significant research gap persists, however, as many studies address emissions and deposition in isolation or focus on specific N_r species or source sectors. For example, previous works have separately quantified NH_3 emissions in the Yangtze River Delta[21], NO_x from vehicles in the Beijing-Tianjin-Hebei region[22], and bulk N_r deposition patterns across China[23]. While insightful, these fragmented approaches preclude a holistic understanding of the complete N_r budget at regional or watershed scales, thereby limiting insights into the net environmental impact and the potential for long-range transport of surplus N_r.

The Erhai Lake Basin (ELB) in southwestern China, a typical plateau lake basin, provides a critical and timely setting for such an integrated budget analysis. Designated as a key demonstration zone for sustainable agriculture and ecological conservation, the ELB has experienced substantial regulatory transformations since 2018. These include a ban on nitrogen- and phosphorus-based chemical fertilizers, the phase-out of high-input cropping systems, and the relocation of intensive livestock operations[24]. These policy interventions have presumably reshaped regional N_r fluxes, but a

comprehensive assessment of their impact on the atmospheric N_r budget is currently absent. While prior research has yielded valuable preliminary data, such as quantifying the contribution of atmospheric deposition (approximately 17%) to the lake's annual nitrogen load[25] and documenting specific agricultural N_r losses[26]. A holistic budget that integrates emissions from all key anthropogenic sources with spatially explicit deposition data is still missing. To bridge this knowledge gap, the current study was designed with three primary objectives: (1) to systematically estimate NH_3 and NO_x emissions from all major sources for the year 2022; (2) to quantify dry and wet N_r deposition across nine representative monitoring sites in 2023; and (3) to establish a comprehensive N_r budget for the entire ELB and its sub-regions. The present work aims to deepen the understanding of nitrogen cycling in fragile plateau lake ecosystems, and to provide a scientific foundation for devising effective regional pollution control strategies.

Materials and methods

Study region

The Erhai Lake Basin (ELB) (25°37'–25°58' N, 99°52'–100°16' E) is located on the Yunnan Plateau in southwestern China, with an average elevation of approximately 1,900 m above sea level (Fig. 1a, b). This basin represents a typical low-altitude plateau lake catchment, characterized by a mean annual temperature of 15.1 °C and a mean annual precipitation of 1,000 mm[27]. The ELB encompasses 18 townships, and supports a total population of approximately 0.9 million. The basin features a diverse landscape, including intensive agricultural and livestock production zones, urban centers, and tourist areas. Key townships include Sanying, Zibihu, and Yousuo for agriculture and livestock, and Dali and Shuanglang for tourism[28].

NH_3-N and NO_x-N emissions

A comprehensive emission inventory was compiled for NH_3-N and NO_x-N in the ELB. The primary sources of NH_3-N included livestock, farmland ecosystem, vehicles, waste treatment, biomass burning, fuel combustion, and human excreta. NO_x-N emissions were estimated from vehicles, livestock, farmland ecosystem, biomass burning, and fuel combustion (for a complete list of sub-categories, see Supplementary Table S1). The emissions for each sub-category were calculated by multiplying the corresponding emission factors (EFs) by the relevant activity data[21]:

$$E = \sum_i \sum_j \left(A_{ij} \times EF_{ij}\right) \tag{1}$$

where, E is the total emission of NH_3-N or NO_x-N; i and j denote the major source category and its sub-categories, respectively; A_{ij} is the activity data; EF_{ij} is the corresponding emission factor. EFs were carefully selected from Chinese technical guidelines[30]. For sources not covered by these guidelines, EFs derived from field measurements in geographically and climatically similar regions are applied (see Supplementary Table S2)[16].

This emission inventory was prepared for 2022. The atmospheric deposition monitoring was conducted in 2023. This one-year temporal offset was necessitated by the delay in publishing the official statistical yearbooks for 2023, which are the primary source of reliable activity data. It was asserted that the fundamental structure of emission sources and the intensity of key activities were stable between these two years, as no major policy shifts or structural economic changes were reported. Consequently, the 2022 emission inventory serves as a robust baseline for characterizing the N_r emission profile of the basin and for constructing an annual budget in conjunction with the 2023 deposition measurements.

Livestock emissions

Livestock NH_3-N emissions primarily originated from manure manage-

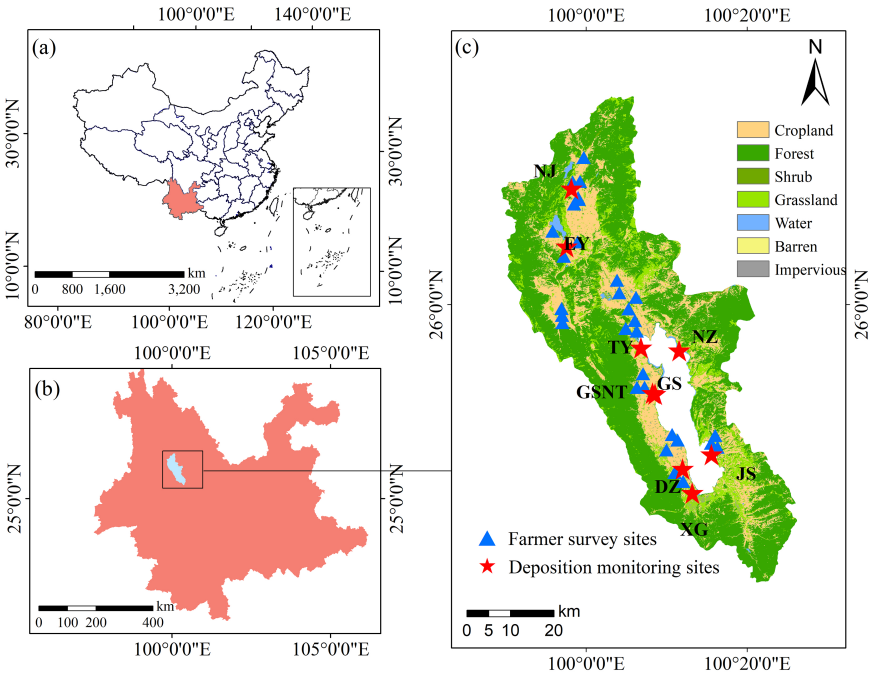

Fig. 1 Location of the study area. (**a**) Yunnan Province within China, (**b**) the Erhai Lake Basin (ELB) within Yunnan, and (**c**) spatial distribution of farmland survey sites and atmospheric nitrogen deposition monitoring sites overlaid on the major land-use types within the ELB[29]. The nine atmospheric deposition monitoring sites (GS, TY, NZ, JS, XG, EY, NJ, GSNT, and DZ) correspond to Gusheng Village, Taoyuan Village, Nanzhao Island, Jinsuo Island, Xiaguan Town, Eryuan County, Niujie Town, Gusheng Cropland, and Dazhuang Village, respectively.

ment. A pivotal local policy enacted in 2018, which prohibited synthetic fertilizers and promoted organic alternatives, has led to the near-comprehensive recycling of livestock manure onto farmland within the ELB. To prevent double-counting of emissions between the livestock and farmland sectors, a mass-flow approach was adopted. This method tracks nitrogen through sequential manure management stages, attributing emissions from manure application to the farmland ecosystem[31].

Emissions were categorized by rearing system: outdoor (direct emissions from grazing) and indoor. Indoor systems were further divided into three management stages: housing (volatilization within barns), storage (volatilization during manure storage), and field application (volatilization after spreading). The emissions for 11 livestock categories were estimated. For animals with a rearing cycle longer than one year (e.g., beef cattle, sows), the year-end stock population was used. For animals with an annual cycle (e.g., broilers), the annual slaughter count was applied. Livestock NH_3 emissions were calculated using Eq. (2):

$$E_l = \sum_i (A_i \times EF_i \times \gamma) \tag{2}$$

where, E_l is the total NH_3-N emission from livestock; A_i is the total ammonia nitrogen (TAN) production; EF_i is the NH_3 emission factor for each manure type and management stage; and γ is the conversion factor from nitrogen to NH_3 (1.214[30]).

Daily TAN production was calculated from the daily excrement volume, nitrogen content, and the TAN fraction (see Supplementary Text S1 for details). The present analysis distinguished between free-range and intensive rearing systems. Emission factors for the housing stage were referenced for the local temperature range of 10–20 °C. It is important to note that the estimate of NO_x-N emissions from livestock only included processes concomitant with NH_3-N emissions (i.e., from manure), and may therefore represent a lower-bound estimate. All livestock parameters and stage-specific EFs are provided in Supplementary Table S3.

Farmland ecosystem emissions

Emissions from farmland ecosystems were estimated for ten major crops (wheat, soybean, potato, barley, rice, corn, rapeseed, tobacco, vegetables, and fruit trees). High-resolution data on nitrogen management practices were obtained through a comprehensive survey of 232 farmers across the ELB in 2022 (Fig. 1c).

A critical adjustment was implemented to avoid double-counting NH_3-N emissions between the livestock and farmland sectors. The amount of externally applied organic fertilizer for each crop was calculated by subtracting the nutrient contribution from locally recycled livestock manure from the total organic fertilizer application reported in the surveys, following Eq. (3):

$$A_i = C_i \times (\varphi_i - \omega_i) \tag{3}$$

where, A_i represents the adjusted total fertilizer application rate for crop i; C_i is the planting area of crop i[28]; φ_i denotes the surveyed fertilizer application rate per unit area (Supplementary Table S4); and ω_i refers to the manure nutrient allocation per unit area for crop i (Supplementary Table S5).

This approach ensures that NH_3 emissions from manure application are attributed to the farmland ecosystem, while emissions from housing and storage stages are retained in the livestock sector.

Furthermore, NH_3-N emissions from straw composting were estimated for eight major crops (excluding vegetables and fruit trees). This calculation incorporated crop yield data, survey-derived straw-to-grain ratios, the fraction of straw used for composting, and regional emission factors[32] (see Supplementary Tables S5 and S6 for parameters).

Finally, direct NH_3-N emissions from cropland soils and biological nitrogen fixation (from soybean cultivation) were included. These were estimated by multiplying the respective cultivation areas by their corresponding emission factors: 0.008 kg N ha^{-1} yr^{-1} for soil emissions, and 0.005 kg N ha^{-1} yr^{-1} for nitrogen-fixing crops[30]. A complete list of EFs used for the farmland ecosystem is provided in Supplementary Table S7.

Vehicular emissions

Vehicular emissions were estimated for nine vehicle types. Although emissions occur from both tailpipes and evaporative processes, tailpipe emissions represent the dominant source of N_r. Vehicle population data (VP_j) for the ELB were compiled from provincial and local traffic management statistics[33]. The average annual mileage (VKT_j) for each vehicle type was obtained from the national technical guideline[34]. Emission factors (EF_j) for NH_3 and NO_x for different vehicle categories were obtained from a combination of these guidelines and recent literature[16] (see Supplementary Table S8 for details). Total vehicular N_r emissions were calculated using Eq. (4):

$$E_v = \sum_j VP_j \times VKT_j \times EF_j \tag{4}$$

where, E_v is the total vehicular N_r emissions.

Biomass burning emissions

Emissions from biomass burning, encompassing straw burning and forest fires, were estimated for NH_3 and NO_x. For straw burning, eight major crops were considered, and emissions were calculated using Eq. (5):

$$E_s = \sum_i Y_i \times N_i \times R_i \times F_i \times EF_i \tag{5}$$

where, E_s is the total N_r emissions from straw burning; Y_i is the annual yield of crop i; N_i is the straw-to-grain ratio; R_i is the proportion of straw subjected to open burning; F_i is the burning efficiency; and EF_i represents the crop-specific emission factor. All parameters and data sources are provided in Supplementary Table S6.

Emissions from forest fires were calculated using Eq. (6):

$$E_f = AR \times D \times F \times EF \tag{6}$$

where, E_f is NH_3 or NO_x emission from forest fires; AR is the annual burned area (km^2), obtained from local yearbooks; D is the dry biomass density (98 t km^{-2}) for the predominant mixed coniferous-broadleaf forests; F is the combustion factor (0.5)[32]; and EF is the respective emission factor.

Other emission sources

NH_3 emissions from waste treatment were categorized into three sub-sectors: sewage treatment, solid waste landfill, and solid waste incineration. Corresponding activity data were collected from local statistical yearbooks, and emission factors were obtained from the technical guidelines[30]. Emissions from fuel combustion were estimated by multiplying fuel consumption by their respective fuel-specific emission factors. Emissions from human excreta were calculated based on the population lacking access to sanitary latrines and the corresponding per capita emission factor. All parameters, emission factors, and references for these sources are listed in Supplementary Tables S2 and S9.

Spatial allocation of emissions

To create a high-resolution spatial distribution map, N_r emissions from the key sources (agriculture and vehicles) were allocated at the township level. Livestock numbers, crop areas, and fertilizer application rates were spatially disaggregated using local statistical yearbooks and the farm survey data. Vehicular emissions were distributed using a GIS-based approach, with the road length of seven different road types

(motorways, trunk, primary, secondary, tertiary, unclassified, and residential roads) serving as a spatial proxy[35]. Road network data were extracted from OpenStreetMap (Supplementary Fig. S1).

Atmospheric N_r deposition

Atmospheric N_r deposition was quantified using a monitoring network of nine sites within the ELB, selected to represent diverse underlying surfaces (e.g., cropland, village, lake island) in 2023 (Fig. 1c; for site details see Supplementary Table S10 and Supplementary Text S2). The dataset for this period incorporates previously published data from January to August[25], complemented by data from the remaining months collected and analyzed in this study to form a complete annual record.

Dry deposition flux estimation

Dry deposition fluxes of gaseous NH_3, NO_2, HNO_3, and particulate NH_4^+ (PNH_4^+), and NO_3^- (PNO_3^-) were estimated using an inferential approach. This approach combines measured atmospheric concentrations of N_r species with modeled monthly dry deposition velocities (V_d), as defined in Eq. (7)[36,12]:

$$F_d = C_d^i \times V_d^i \tag{7}$$

where, F_d is the dry deposition flux (kg N ha^{-1}) of N_r species i over the sampling period; C_d^i represents the atmospheric concentration (μg N m^{-3}) of species i; and V_d^i denotes the corresponding monthly dry deposition velocity (m s^{-1}). The monthly V_d for each species and site was simulated using the Weather Research and Forecasting model coupled with Chemistry (WRF-Chem), version 4.5.1. The model calculates V_d using a resistance-in-series scheme, which depends on surface characteristics such as land use and aerodynamic roughness. The application and evaluation of this model for various land-use types in the ELB have been documented previously[25], and the resulting monthly V_d values are presented in Supplementary Fig. S2 (see Supplementary Text S3 for further details).

Monthly mean concentrations of NH_3, HNO_3, PNH_4^+, and PNO_3^- were measured using the Denuder for Long-Term Atmospheric (DELTA) sampling system. Monthly mean NO_2 concentrations were determined using Gradko passive sampling tubes[12]. Detailed protocols for sampler operation, sample extraction, and chemical analysis are provided in Supplementary Text S4. This study quantified dry deposition for inorganic N_r species only; organic nitrogen was not included.

Wet deposition flux estimation

Wet deposition samples were collected on a per-event basis using APS-3B automatic rainfall collectors (Changsha Xianglan Equipment Inc., China). Standard protocols for instrument operation, sample collection, and pretreatment were adhered to, as described by Shen et al.[37]. Total wet N_r deposition was calculated as the sum of ammonium nitrogen (NH_4^+-N), nitrate nitrogen (NO_3^--N), dissolved organic nitrogen (DON), and particulate nitrogen (PN) in the precipitation. Although PN may include a fraction from crustal dust, it also incorporates nitrogen derived from atmospheric N_r species; thus, its inclusion offers a more comprehensive assessment of total nitrogen input via precipitation. Analytical methods for each N_r species are detailed in Supplementary Text S5. Wet deposition was monitored at seven of the nine sites; the GSNT and DZ sites were excluded due to their proximity (< 5 km) to the GS station to avoid spatial overlap.

The volume-weighted mean (VWM) concentration for each N_r species was calculated for monthly and annual periods using Eq. (8):

$$C_{VWM} = \sum_{i=1}^{k}(C_i \times P_i) / \sum_{i=1}^{k} P_i \tag{8}$$

where, C_{vwm} is the VWM concentration (mg N L^{-1}); C_i represents the concentration in the i-th precipitation sample; P_i denotes the rainfall depth (mm) for the i-th event; and k is the total number of samples in the period.

The wet deposition flux was subsequently calculated using Eq. (9)

$$F_w = C_{VWM} P_t / 100 \tag{9}$$

where, F_w is the wet deposition flux (kg N ha^{-1}); P_t is the total precipitation (mm) for the period; and 100 is the unit conversion factor.

Quality assurance and quality control

The accuracy of the analytical methods was verified using standard reference materials. Recovery rates for total nitrogen (TN), NH_4^+-N, and NO_3^--N were 92%–126%, 88%–106%, and 91%–112%, respectively (Supplementary Fig. S3). To ensure precision, all dry deposition filters and precipitation samples were analyzed in triplicate. Final concentrations and fluxes are reported as the mean ± standard deviation, with the relative standard deviation for all replicates being less than 10%.

Statistical analysis

One-way analysis of variance (ANOVA) followed by Duncan's post-hoc test was employed to identify statistically significant differences in N_r species concentrations, and fluxes across temporal (e.g., monthly, seasonal) and spatial scales. All descriptive statistical analyses and graphical work were performed using Origin 9.1 (OriginLab Corporation, USA), and SPSS 11.5 (SPSS Inc., USA).

Results

Characteristics of NH_3 and NO_x emissions

Source contributions

In 2022, the total atmospheric N_r emissions from the ELB were estimated at 10,720.4 tonnes (t), comprising 4,758.6 t of NH_3-N (44.4%), and 5,961.8 t of NO_x-N (55.6%) (Fig. 2).

Agriculture was the dominant source of NH_3-N, collectively contributing 91.7% of the total. The livestock sector was the single largest contributor, emitting 2,328.5 t (48.9% of total NH_3-N), with dairy cattle (843.2 t, 36.2% of livestock emissions), laying hens (22.0%), and hogs (19.2%) being the primary sources. The farmland ecosystem accounted for 2,159.4 t (45.4% of total NH_3-N), overwhelmingly from fertilizer application (94.2% of farmland emissions). Corn, vegetables, fruit trees, soybeans, and rice were the principal crop sources, collectively responsible for 80.9% of fertilization emissions. Emissions from other sources, including vehicles, waste treatment, biomass burning, human waste, and fuel combustion, were minor (collectively < 5.7%) (Fig. 2a; Supplementary Table S11).

In stark contrast, the transportation sector accounted for 98.2% of NO_x-N emissions (5,856.5 t). Contributions from all other sectors (farmland, livestock, biomass burning, and fuel combustion) were negligible (≤ 1% each). Within the vehicle fleet, heavy-duty trucks (HTD, 42.3%), small passenger cars (SPC, 36.1%), and light-duty trucks (LDT, 15.9%) were the primary emitters (Fig. 2b; Supplementary Table S11).

Spatial patterns

The spatial distributions of the dominant emission sources, i.e., NH_3-N from farmland and livestock, and NO_x-N from vehicles, are shown in Fig. 3. Together, these sources represented 96.5% of total N_r emissions.

Emissions of NH_3-N from farmland were concentrated in the townships of Sanying (14.2%), Zibihu (12.6%), and Yousuo (11.0%) (Fig. 3a). Similarly, livestock NH_3-N emissions were highest in Sanying (18.4%), Fengyi (17.2%), Yousuo (12.8%), and Zibihu (11.0%) (Fig. 3b). Consequently, the northern sub-region (Eryuan County)

https://doi.org/10.48130/nc-0025-0018

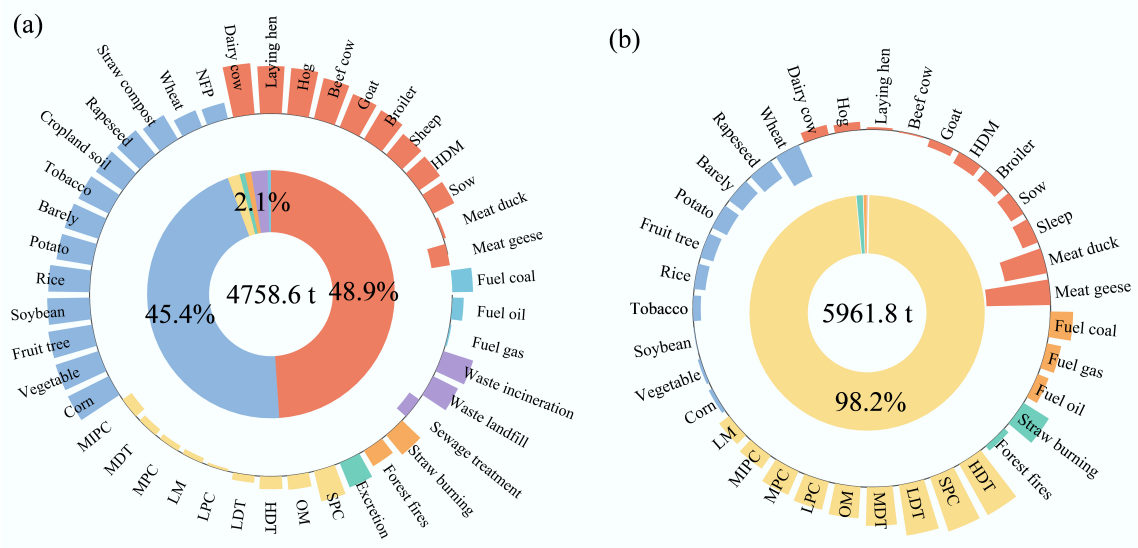

Fig. 2 Source apportionment of (**a**) NH_3-N and (**b**) NO_x-N emissions in the Erhai Lake Basin for 2022. The outer ring displays the emission rates for all sub-categories (bar heights correspond to log-transformed emissions). The inner ring illustrates the proportional contribution of primary sources to the total. LPC, large passenger cars; MPC, medium passenger cars; SPC, small passenger cars; MIPC, mini passenger cars; HTD, heavy-duty trucks; MTD, medium-duty trucks; LTD, light-duty trucks; OM, ordinary motorcycles; LM, light motorcycles; NFP, nitrogen-fixing plants; HDM, horses, donkeys, and mules.

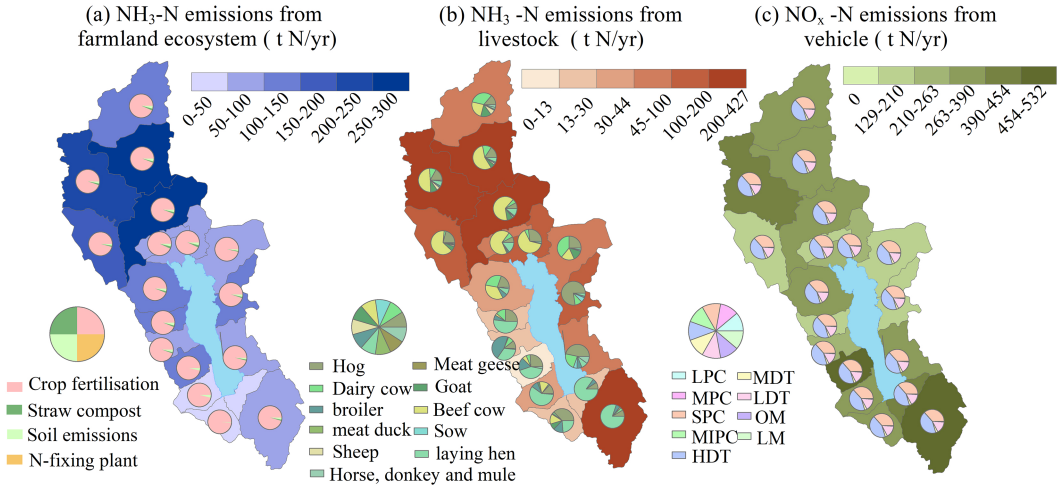

Fig. 3 Spatial distribution of (**a**) NH_3-N emissions from the farmland ecosystem, (**b**) NH_3-N emissions from livestock, and (**c**) NO_x-N emissions from motor vehicles across townships in the Erhai Lake Basin. Emissions are presented as percentages of the total basin-wide emission for each respective source category.

exhibited the most intense NH_3-N emissions, consistent with its predominance of agricultural and livestock activities, in contrast to the more urbanized southern sub-region (Dali).

In contrast, NO_x-N emissions from vehicles were more evenly distributed across the basin, with township contributions ranging from 2.2% to 9.1% (Fig. 3c). The highest contributions were observed in townships with major urban and transportation hubs, including Dali (9.1%), Fengyi (8.6%), Manjiang (7.8%), Zibihu (7.0%), Xiaguan (6.7%), and Taihe (6.3%).

Atmospheric N_r deposition

The annual mean concentrations and deposition fluxes of N_r species across the nine monitoring sites are summarized in Fig. 4. In ambient air, NH_3 and NO_2 were the dominant gaseous species, accounting for 47.5% and 40.9% of the total gaseous N_r concentration, respectively (Fig. 4a). In precipitation, NH_4^+-N was the major component of the volume-weighted mean (VWM) N_r concentration (53.6%), followed by NO_3^--N (21.0%), DON (16.2%), and PN (9.2%) (Fig. 4b).

Dry deposition was overwhelmingly dominated by NH_3, which contributed 74.5% to the total dry flux (Fig. 4c). The composition of wet deposition fluxes generally reflected the VWM concentration pattern (Fig. 4b, d).

Spatially, the annual total N_r deposition averaged 10.4 ± 1.0 kg N ha^{-1} yr^{-1} across the basin, but exhibited considerable variability, ranging from 7.5 kg N ha^{-1} yr^{-1} at the JS site (a lake island with minimal direct influence) to 17.7 kg N ha^{-1} yr^{-1} at the NJ site (subject to combined urban and agricultural emissions) (Supplementary Table S12). Reduced nitrogen (NH_x-N, the sum of NH_3 and NH_4^+) was the dominant form in total deposition, constituting 68.9%. Dry deposition was the primary pathway, accounting for 58.2% of the total flux, compared to 41.8% for wet deposition

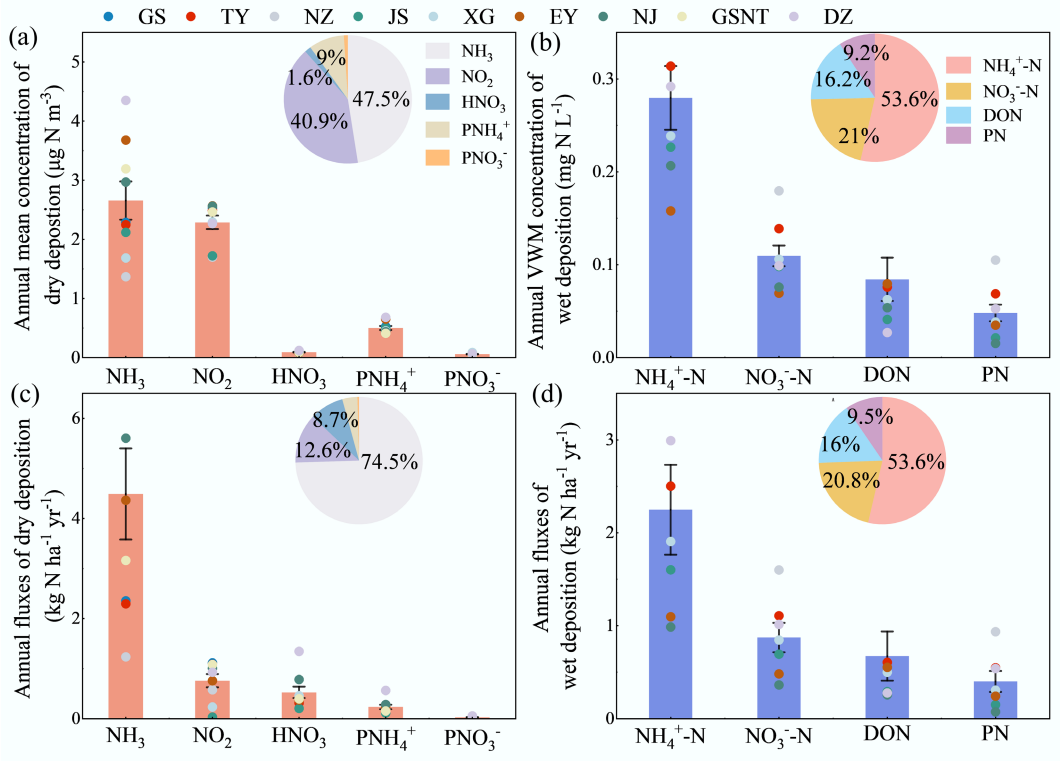

Fig. 4 Annual mean concentration and deposition fluxes of different N_r species in the Erhai Lake Basin (2023). (**a**), (**c**) Dry deposition: concentration and flux. (**b**), (**d**) Wet deposition: volume-weighted mean (VWM) concentration and flux. Data are presented as mean ± standard deviation across nine monitoring sites for dry deposition and seven sites for wet deposition.

(Fig. 5a).

Monthly total N_r deposition fluxes ranged from 0.3 to 2.1 kg N ha^{-1}. NH_3-N was consistently the largest contributor (48.0%), followed by NH_4^+-N (17.4%) and various oxidized nitrogen species (summing to ~23.3%). Seasonally, summer received the highest deposition, accounting for 45.4% of the annual total. Dry deposition was the predominant pathway in spring (75.3%) and winter (88.3%), while wet deposition predominated in summer (52.4%) and autumn (51.2%) (Fig. 5b).

Atmospheric N_r budget

The annual atmospheric N_r budget for the ELB, defined as emissions minus deposition, is presented in Table 1. A substantial surplus was evident for both NH_x-N and NO_y-N at the sub-regional level. The NH_x-N budget was positive in both Dali (1,221.9 t yr^{-1}), and Eryuan (1,779.8 t yr^{-1}), indicating that NH_3 emissions far exceeded reduced nitrogen deposition. Similarly, the NO_y-N budget showed a large surplus of 3,821.7 t yr^{-1} in Dali and 1,599.1 t yr^{-1} in Eryuan.

After accounting for the wet deposition of particulate and organic nitrogen (PN + DON), the total N_r budget (BTN) remained strongly

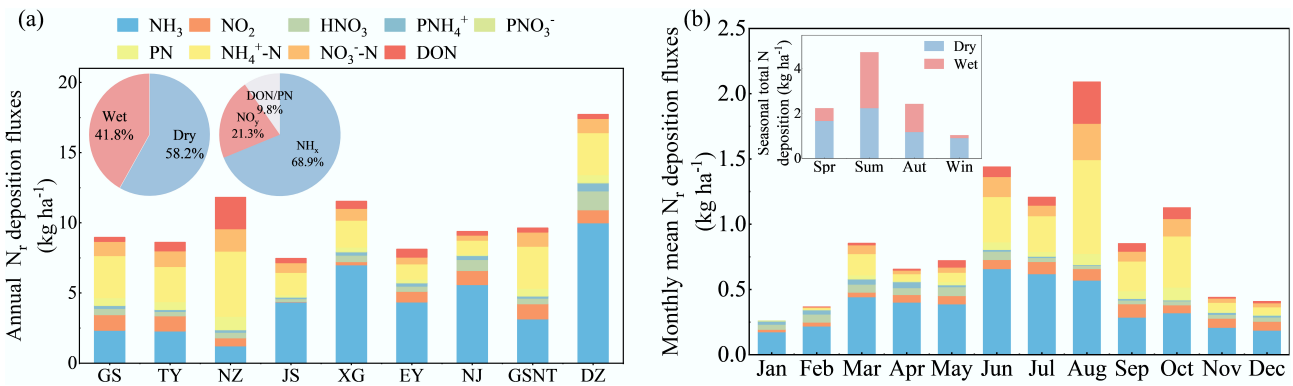

Fig. 5 Composition of atmospheric nitrogen deposition in the Erhai Lake Basin. (**a**) Proportions of different N_r species in the annual total deposition (dry + wet) across all sites. (**b**) Monthly and seasonal variations in the contributions of different N_r species to total deposition, based on the average of all nine monitoring sites. Species groupings: NH_x (sum of NH_4^+, NH_3, and PNH_4^+); NO_y (sum of NO_3^-, NO_2, HNO_3, and PNO_3^-); DON, dissolved organic nitrogen; PN, particulate nitrogen from wet deposition.

https://doi.org/10.48130/nc-0025-0018

Table 1 Atmospheric budgets of NH_x, NO_y, and total N_r for Dali County, Eryuan County, and the entire Erhai Lake Basin (ELB)

Administrative scope	Emission (E t yr^{-1})		Deposition (D t yr^{-1})		Budget (B t yr^{-1})		Budget of Total N_r (t yr^{-1})
	NH_3	NO_x	NH_x	NO_y	NH_x	NO_y	
Dali (DL)	2,209.8	4,130.0	987.9	308.3	1,221.9	3,821.7	4,890.8
Eryuan (EY)	2,548.8	1,831.8	769	232.7	1,779.8	1,599.1	3,310.4
Erhai Lake Basin (ELB)	4,758.6	5,961.8	1,756.9	541	3,001.7	5,420.8	8,201.2

(1) Budget (B) for NH_x and NO_y is calculated as B = E − D. (2) Budget of Total N_r (BTN) is calculated as BTN = (NH_x Budget + NO_y Budget) − (Wet deposition of particulate N + Wet deposition of dissolved organic N). This represents the net atmospheric surplus after accounting for the major deposition pathways of emitted N. (3) DL, EY, and ELB denote Dali County, Eryuan County, and the entire Erhai Lake Basin, respectively.

positive: 4,890.8 t yr^{-1} for Dali and 3,310.4 t yr^{-1} for Eryuan. Integrated across the entire basin, the ELB was a clear net source of atmospheric N_r, with a total surplus of 8,201.2 t yr^{-1}. This net emission was composed of surpluses of 3,001.7 t yr^{-1} for NH_x-N and 5,420.8 t yr^{-1} for NO_y-N. The consistent surpluses across all major nitrogen pools and sub-regions unequivocally demonstrate that the ELB acts as a significant net source of atmospheric reactive nitrogen.

Discussion

Characteristics of high N_r emissions in the Erhai Lake Basin

The present analysis reveals that the ELB is a hotspot of atmospheric N_r emissions. The estimated emission intensities for NH_3-N (18.6 kg ha^{-1} yr^{-1}) and NO_x-N (23.2 kg ha^{-1} yr^{-1}) substantially exceed the national averages and are approximately 2.2 and 2.4 times higher than the corresponding averages for Yunnan Province[38,39]. This finding is robust and corroborated by a local-scale study that reported a similarly high NH_3-N emission intensity (20.3 kg ha^{-1} yr^{-1}) in a sub-catchment of the ELB[40].

Agriculture was the unequivocal dominant source of NH_3-N, responsible for 91.7% of the total. Livestock production (48.9%) and fertilizer application (42.8%) contributed almost equally to the agricultural NH_3 budget (Fig. 2), a pattern consistent with national-scale emission profiles[41]. Within these categories, dairy cattle (36.2% of livestock emissions) and layer hens (22.0%) were the principal livestock sources, while maize (20.2%) and vegetables (18.9%) were the dominant crop sources, aligning with findings from a recent local study[40]. In stark contrast, the transportation sector overwhelmingly dominated NO_x-N emissions (98.2%), primarily from heavy-duty trucks (42.3%) and light-duty passenger vehicles (36.1%). This emission profile is consistent with national vehicle inventories[39], highlighting the growing influence of traffic in the region.

Characteristics and ecological impact of atmospheric deposition in the Erhai Lake Basin

Despite substantial N_r emissions, the corresponding atmospheric deposition flux in the ELB was relatively low. Our measured total N_r deposition (10.4 kg N ha^{-1} yr^{-1}) is consistent with a previous estimate for this basin (10.67 kg N ha^{-1} yr^{-1})[25] but is considerably lower than the national average and values reported for other heavily impacted Chinese lake basins, such as Taihu (64.8 kg N ha^{-1} yr^{-1}) and Dongting (48.0 kg N ha^{-1} yr^{-1})[13,42,43]. It is also lower than deposition fluxes reported for Lake Dianchi, Chaohu, and Qinghai Lake[44−47].

Nevertheless, atmospheric deposition constitutes a critical nitrogen source to Erhai Lake. Historical data indicate that wet deposition contributed 183.3 t N in 2019, accounting for 20.0% of the annual riverine input[48]. Kang et al. estimated total atmospheric deposition to the lake at 218 t N, representing 17% of the total external nitrogen load[25]. The present study yields a comparable total deposition estimate of 277 t N to the lake surface. When viewed against the riverine input, this constitutes a significant contribution of 33.5%[48], a share remarkably similar to that reported for the highly polluted Lake Taihu (33.3%)[42]. This finding underscores that even in regions with moderate per-area deposition, the atmosphere can be a significant pathway for nitrogen loading in aquatic ecosystems, a point critical for managing lake eutrophication.

Environmental implications of atmospheric N_r budgets in the Erhai Lake Basin

The atmospheric N_r budget unequivocally identifies the ELB as a substantial net source to the atmosphere. Local deposition offset only 23.5% of total emissions, revealing a stark contrast between the fate of reduced and oxidized nitrogen: 36.9% of emitted NH_x was deposited locally, compared to a mere 9.1% of emitted NO_y. This indicates that a large fraction of the emitted N_r, particularly NO_y, is exported from the basin[49]. The dominance of reduced nitrogen in deposition, despite higher NO_y emissions, is explained by two key factors: firstly, the higher local deposition-to-emission ratio for NH_x; and secondly, a national-scale shift towards reduced N deposition, driven by more effective NO_x control policies compared to less regulated agricultural NH_3 emissions.

The exceptionally low deposition-to-emission ratio is likely a consequence of the unique 'alpine-lake-valley' topography. This complex terrain drives a robust diurnal mountain-valley breeze circulation. We hypothesize that this circulation entraps air masses, including N_r species, in periodic vertical loops[36,49], thereby prolonging their atmospheric residence time. This mechanism enhances the potential for long-range transport of pollutants, particularly the more stable NO_y compounds, over immediate local deposition. Furthermore, the extended residence time provides a crucial window for the formation of secondary particulate matter (e.g., ammonium nitrate and sulfate) in the atmosphere, potentially exacerbating regional fine particulate pollution downwind[50,51].

The spatial decoupling between emissions and deposition is a common phenomenon in atmospheric chemistry. Globally, a significant portion of terrestrially emitted N_r is transported and deposited in marine ecosystems[15]. Our finding of a low local retention (23.5%) is more pronounced than the 44.7% reported for another subtropical agricultural watershed[15], highlighting the unique efficiency of the ELB in exporting N_r. This is further supported by a spatial correlation analysis between township-level emission intensities and deposition fluxes at nearby sites, which showed no significant positive relationship (Supplementary Fig. S4). This lack of correlation corroborates that local emission hotspots do not necessarily dictate local deposition patterns, reinforcing the hypothesis that the complex circulation facilitates the export of a large fraction of emitted N_r from the basin.

Uncertainty analysis

Several sources of uncertainty in the budget calculation warrant discussion. The most apparent is the temporal discrepancy between the emission (2022) and deposition (2023) inventories, necessitated by data availability. However, it was found that this does not invalidate the core conclusion of a significant net source, as no major structural changes in emission sources occurred between these years, and the calculated surplus (8,201.2 t N yr^{-1}) is too substantial to be bridged by inter-annual variability alone. Furthermore, the inclusion of PN in wet deposition might lead to a slight overestimation, as PN can contain non-reactive nitrogen from crustal dust.

The emission inventories are subject to uncertainties in both activity data and EFs. Activity data, sourced from official statistics and detailed surveys, are associated with relatively low uncertainty (CV ~5%–10%). In contrast, EFs, primarily derived from the literature rather than localized measurements, contribute more significantly to the overall uncertainty[16]. Error propagation analysis estimated the total uncertainties at ± 10.6% for NH_3 and ± 11.4% for NO_x, the latter dominated by the vehicle sector (see Supplementary Text S6 and Supplementary Tables S13–S19)[52].

The deposition estimates also have potential biases. The monitoring network, while representative of major land-use types, may not fully capture deposition in underrepresented areas such as forests, potentially leading to spatial averaging bias. Our dry deposition estimate does not include organic nitrogen, which has been reported to constitute about 1.1% of total dry N deposition in this region[25]. Additionally, the inferential method for dry deposition, particularly for NH_3, is subject to uncertainty due to the complex, bi-directional nature of ammonia exchange[20].

While this study represents a significant advancement in quantifying the N_r budget for a plateau lake basin, future work should prioritize developing localized EFs, incorporating organic N into dry deposition measurements, and applying chemical transport models to better constrain the fate of exported N_r.

Conclusions

This study establishes the comprehensive atmospheric N_r budget for the ELB, a representative subtropical plateau lake ecosystem in China. The present analysis unequivocally demonstrates that the ELB is a significant net source of atmospheric N_r, with annual emissions of 10,720.4 t far surpassing local deposition, yielding a substantial budget surplus of 8,201.2 t N yr^{-1}. Source apportionment revealed a clear divergence: NH_3-N emissions were overwhelmingly agricultural in origin (91.7%), with nearly equal contributions from livestock farming (48.9%) and synthetic fertilizer application (42.8%). In contrast, NO_x-N emissions were almost entirely (98.2%) attributable to the transportation sector. Atmospheric deposition, averaging 10.4 kg N ha^{-1} yr^{-1}, was predominantly in the form of reduced nitrogen (NH_x-N, 68.9%). The pronounced net emission status, likely enhanced by the unique 'alpine-lake-valley' topography that promotes pollutant export, highlights the imperative for integrated mitigation strategies. Effective policy must concurrently address both primary sources: through improved manure management and precision fertilization in agriculture, and via the promotion of clean vehicles and stricter emission standards in transportation.

To refine future assessments and quantify the downstream impacts, three research priorities are recommended: (1) development of locally validated emission factors; (2) inclusion of organic nitrogen in comprehensive deposition monitoring; and (3) application of chemical transport models to track the regional fate and environmental consequences of the exported N_r.

Supplementary information

It accompanies this paper at: https://doi.org/10.48130/nc-0025-0018.

Ethical statements

Not applicable.

Author contributions

The authors confirm their contributions to the paper as follows: Qikun Shen: analysis and interpretation of results; Bowen Tang: methodology; Xinyu Wu, Jiahui Kang: data collection; Qikun Shen, Bowen Tang, Xinyu Wu: draft manuscript preparation and figure visualization; Jiawei Li, Yuepeng Pan, Xuejun Liu: writing – review and guidance; Wen Xu: study conception and design and draft revision. All authors were involved in the discussion of the data, and the revision of the manuscript.

Data availability

The datasets used or analyzed during the current study are available from the corresponding author upon reasonable requests.

Funding

This work was supported by the Major Science and Technology Project of Yunnan Province (Grant No. 202202AE090034), the National Natural Science Foundation of China (Grant No. 42175137), and the National Key Research and Development Program of China (Grant No. 2021YFD1700902).

Declarations

Competing interests

The authors declare that they have no conflict of interest.

Author details

[1]College of Resources and Environmental Sciences, National Academy of Agriculture Green Development, Key Laboratory of Plant–Soil Interactions, Ministry of Education, National Observation and Research Station of Agriculture Green Development (Quzhou, Hebei), China Agricultural University, Beijing 100193, China; [2]Key Laboratory of Regional Climate-Environment for Temperate East Asia (RCE-TEA), Institute of Atmospheric Physics (IAP), Chinese Academy of Sciences (CAS), Beijing 100029, China; [3]State Key Laboratory of Atmospheric Boundary Layer Physics and Atmospheric Chemistry, Institute of Atmospheric Physics, Chinese Academy of Sciences, Beijing 100029, China

References

[1] Erisman JW, Hensen A, de Vries W, Kros H, van de Wal T, et al. 2002. NitroGenius: a nitrogen decision support system. *AMBIO: A Journal of the Human Environment* 31(2):190–196

[2] Wang G, Zhang R, Gomez ME, Yang L, Zamora ML, et al. 2016. Persistent sulfate formation from London Fog to Chinese haze. *Proceedings of the National Academy of Sciences of the United States of America* 48(113):13630–13635

[3] Zhang R, Wang G, Guo S, Zamora ML, Ying Q, et al. 2015. Formation of urban fine particulate matter. *Chemical Reviews* 115(10):3803–3855

[4] Meng F, Zhang Y, Kang J, Heal MR, Reis S, et al. 2022. Trends in secondary inorganic aerosol pollution in China and its responses to

emission controls of precursors in wintertime. *Atmospheric Chemistry Physics* 22:6291–6308
[5] Karthick Raja Namasivayam S, Priyanka S, Lavanya M, Krithika Shree S, Francis AL, et al. 2024. A review on vulnerable atmospheric aerosol nanoparticles: sources, impact on the health, ecosystem and management strategies. *Journal of Environmental Management* 365:121644
[6] Shi Y, Cui S, Ju X, Cai Z, Zhu Y. 2015. Impacts of reactive nitrogen on climate change in China. *Scientific Reports* 5:8118
[7] Lin BL, Kumon Y, Inoue K, Tobari N, Xue M, et al. 2021. Increased nitrogen deposition contributes to plant biodiversity loss in Japan: insights from long-term historical monitoring data. *Environmental Pollution* 290:118033
[8] Feng S, Wang M, Heal MR, Liu X, Liu X, et al. 2024. The impact of emissions controls on atmospheric nitrogen inputs to Chinese river basins highlights the urgency of ammonia abatement. *Science Advances* 10:2558
[9] Liu X, Du E. 2020. *Atmospheric reactive nitrogen in China. Part I: reactive nitrogen emission and deposition in China*. Singapore: Springer doi: 10.1007/978-981-13-8514-8
[10] Schlesinger WH. 2009. On the fate of anthropogenic nitrogen. *Proceedings of the National Academy of Sciences of the United States of America* 106(1):203–208
[11] Zheng B, Tong D, Li M, Liu F, Hong C, et al. 2018. Trends in China's anthropogenic emissions since 2010 as the consequence of clean air actions. *Atmospheric Chemistry and Physics* 18(19):14095–14111
[12] Xu W, Luo XS, Pan YP, Zhang L, Tang AH, et al. 2015. Quantifying atmospheric nitrogen deposition through a nationwide monitoring network across China. *Atmospheric Chemistry and Physics* 15:12345–12360
[13] Liu L, Wen Z, Liu S, Zhang X, Liu X. 2024. Decline in atmospheric nitrogen deposition in China between 2010 and 2020. *Nature Geoscience* 17(8):733–736
[14] Zhang L, Chen Y, Zhao Y, Henze DK, Zhu L, et al. 2018. Agricultural ammonia emissions in China: reconciling bottom-up and top-down estimates. *Atmospheric Chemistry and Physics* 18:339–355
[15] Fowler D, Coyle M, Skiba U, Sutton MA, Cape JN, et al. 2013. The global nitrogen cycle in the twenty-first century. *Philosophical Transactions of the Royal Society B: Biological Sciences* 368(1621):20130164
[16] Zhu X, Shen J, Li Y, Liu X, Xu W, et al. 2021. Nitrogen emission and deposition budget in an agricultural catchment in subtropical Central China. *Environmental Pollution* 289:117870
[17] Li M, Liu H, Geng G, Hong C, Liu F, et al. 2017. Anthropogenic emission inventories in China: a review. *National Science Review* 4(6):834–866
[18] Ning X, Li J, Zhuang P, Lai S, Zheng X. 2024. Wildfire combustion emission inventory in Southwest China (2001–2020) based on MODIS fire radiative energy data. *Atmospheric Pollution Research* 15(11):102279
[19] Zhao Y, Li B, Dong J, Li Y, Wang Y, et al. 2023. Improved ammonia emission inventory of fertilizer application for three major crops in China based on phenological data. *Science of The Total Environment* 896:165225
[20] Zhang Q, Li Y, Wang M, Wang K, Meng F, et al. 2021. Atmospheric nitrogen deposition: a review of quantification methods and its spatial pattern derived from the global monitoring networks. *Ecotoxicology and Environmental Safety* 216:112180
[21] Yu X, Shen L, Hou X, Yuan L, Pan Y, et al. 2020. High-resolution anthropogenic ammonia emission inventory for the Yangtze River Delta, China. *Chemosphere* 251:126342
[22] Zhu C, Qu X, Qiu M, Zhu C, Wang C, et al. 2023. High spatiotemporal resolution vehicular emission inventory in Beijing-Tianjin-Hebei and its surrounding areas (BTHSA) during 2000–2020, China. *Science of The Total Environment* 873:162389
[23] Wen Z, Wang R, Li Q, Liu J, Ma X, et al. 2022. Spatiotemporal variations of nitrogen and phosphorus deposition across China. *Science of The Total Environment* 830:154740
[24] Hou Y, Xu W, Cong WF, Jin K, Xu J, et al. 2023. Agricultural green development in the Erhai Lake Basin — the way forward. *Frontiers of Agricultural Science and Engineering* 10(4):510–517
[25] Kang J, Du X, Tang B, Shen Q, Li J, et al. 2025. Wet and dry deposition of atmospheric nitrogen to Lake Erhai basin: composition, spatiotemporal patterns and implications for nitrogen inputs into the lake. *Atmospheric Environment* 345:120995
[26] Zou T, Meng F, Zhou J, Ying H, Liu X, et al. 2023. Quantifying nitrogen and phosphorus losses from crop and livestock production and mitigation potentials in Erhai Lake Basin, China. *Agricultural Systems* 211:103745
[27] Ji N, Wang S, Zhang L. 2017. Characteristics of dissolved organic phosphorus inputs to freshwater lakes: a case study of Lake Erhai, southwest China. *Science of The Total Environment* 601-602:1544–1555
[28] National Bureau of Statistics of China, Dali Survey Team (NBSC). 2022. *Dali Statistical Yearbook*. China Statictics Press, Dali, China (in Chinese)
[29] Yang J, Huang X. 2021. The 30 m annual land cover dataset and its dynamics in China from 1990 to 2019. *Earth System Science Data* 13(8):3907–3925
[30] Ministry of Ecology and Environment of the People's Republic of China (MEE). 2014. *Technical guidelines for the compilation of atmospheric ammonia source emission inventories (for trial implementation)*. MEE, China (in Chinese)
[31] Zhu C, Li R, Qiu M, Zhu C, Gai Y, et al. 2024. High spatiotemporal resolution ammonia emission inventory from typical industrial and agricultural province of China from 2000 to 2020. *Science of The Total Environment* 918:170732
[32] Ministry of Ecology and Environment of the People's Republic of China (MEE). 2014. *Technical guideline for the compilation of air pollutant emission inventory from biomass combustion sources (for trial implementation)*. MEE, China (in Chinese)
[33] National Bureau of Statistics of China, Dali Survey Team (NBSC). 2022. *Yunnan Statistical Yearbook*. China Statictics Press, Dali, China (in Chinese)
[34] Ministry of Ecology and Environment of the People's Republic of China (MEE). 2014. *Technical guideline for compiling the air pollutant emission inventory of road motor vehicles (for trial implementation)*. MEE, China (in Chinese)
[35] Gómez CD, González CM, Osses M, Aristizábal BH. 2018. Spatial and temporal disaggregation of the on-road vehicle emission inventory in a medium-sized Andean city. Comparison of GIS-based top-down methodologies. *Atmospheric Environment* 179:142–155
[36] Serafin S, Adler B, Cuxart J, De Wekker SFJ, Gohm A, et al. 2018. Exchange processes in the atmospheric boundary layer over mountainous terrain. *Atmosphere* 9:102
[37] Shen Q, Du X, Kang J, Li J, Pan Y, et al. 2024. Atmospheric wet and dry phosphorus deposition in Lake Erhai, China. *Environmental Pollution* 355:124200
[38] Zhi G, Du J, Chen A, Jin W, Ying N, et al. 2024. Progression of an emission inventory of China integrating CO_2 with air pollutants: a chance to learn the influence of development on emissions. *Atmospheric Environment* 316:120184
[39] Gao Y, Zhang L, Huang A, Kou W, Bo X, et al. 2022. Unveiling the spatial and sectoral characteristics of a high-resolution emission inventory of CO_2 and air pollutants in China. *Science of The Total Environment* 847:157623
[40] Wu X, Kang J, Du X, Shen Q, Feng J, et al. 2024. Study on characteristics of cropland ammonia emissions and its near-source deposition in typical small watershed of plateau lake. *Ecology and Environmental Sciences* 33(08):1236–1244 (in Chinese)
[41] Li B, Chen L, Shen W, Jin J, Wang T, et al. 2021. Improved gridded ammonia emission inventory in China. *Atmospheric Chemistry and Physics* 21(20):15883–15900
[42] Ti C, Gao B, Luo Y, Wang S, Chang SX, et al. 2018. Dry deposition of N has a major impact on surface water quality in the Taihu Lake region in southeast China. *Atmospheric Environment* 190:1–9
[43] Zhang Y, Liu C, Liu X, Xu W. 2019. Atmospheric nitrogen deposition around the Dongting Lake, China. *Atmospheric Environment* 207:197–204

[44] Zhang X, Lin C, Zhou X, Lei K, Guo B, et al. 2019. Concentrations, fluxes, and potential sources of nitrogen and phosphorus species in atmospheric wet deposition of the Lake Qinghai Watershed, China. *Science of The Total Environment* 682:523−531

[45] Zhan X, Bo Y, Zhou F, Liu X, Paerl HW, et al. 2017. Evidence for the importance of atmospheric nitrogen deposition to eutrophic Lake Dianchi, China. *Environmental Science & Technology* 51(12):6699−6708

[46] Li W, Wang X, Song W, Zhang Z, Wang X, et al. 2025. On the contribution of atmospheric reactive nitrogen deposition to nitrogen burden in a eutrophic Lake in Eastern China. *Water Research* 268:122597

[47] Zhang X, Lin C, E C, Liu X. 2022. Atmospheric dry deposition of nitrogen and phosphorus in Lake Qinghai, Tibet Plateau. *Atmospheric Pollution Research* 13(7):101481

[48] Huang M. 2022. Water quality characteristics and pollution load estimation of main rivers around Erhai Lake. *Yangtze River* 53(1):61−66 (in Chinese)

[49] Cooper OR, Parrish DD, Stohl A, Trainer M, Nédélec P, et al. 2010. Increasing springtime ozone mixing ratios in the free troposphere over western North America. *Nature* 463(7279):344−348

[50] Lang MN, Gohm A, Wagner JS. 2015. The impact of embedded valleys on daytime pollution transport over a mountain range. *Atmospheric Chemistry and Physics* 15(20):11981

[51] Li X, Zhang C, Liu P, Liu J, Zhang Y, et al. 2020. Significant influence of the intensive agricultural activities on atmospheric $PM_{2.5}$ during autumn harvest seasons in a rural area of the North China Plain. *Atmospheric Environment* 241:117844

[52] IPCC. 1997. Quantifying uncertainties in practice. In *Good Practice Guidance and Uncertainty Management in National Greenhouse Gas Inventories*. IES, IPCC, OECD, Bracknell

Copyright: © 2026 by the author(s). Published by Maximum Academic Press, Fayetteville, GA. This article is an open access article distributed under Creative Commons Attribution License (CC BY 4.0), visit https://creativecommons.org/licenses/by/4.0/.